E3S Web of Conferences **460**, 04024 (2023) https://doi.org/10.1051/e3sconf/202346004024
BFT-2023

Development unit removal and signal transmission for information - measuring system of electrical impedance tomography of biological objects

G.K. Aleksanyan[1], *A.I.* Kucher[1], *N.I.* Gorbatenko[1], and *M.C.* Nguyen[2]

[1] Platov South-Russian State Polytechnic University (NPI), 132 Prosveshcheniya St., Rostov region, Novocherkassk, Russian Federation
[2] Le Quy Don Technical University, 236 Hoang Quoc Viet, Ha Noi, Viet Nam

Abstract. The article is devoted to the development of a unit for collecting, primary processing and transmitting measurement information for electrical impedance tomography tasks. The developed block provides the ability to connect one of the terminals of the current source to a common point, and the second terminal to any of the electrodes on the surface of the biological object under study; provides the ability to measure the amplitude of potential changes on any of the electrodes on the surface of a biological object relative to a common point. Control is carried out using a control program installed on a personal computer, connected to it via a universal USB port. It is possible to control the current source (amplitude, shape and frequency) through voltage. An experimental verification of the accuracy of generating a control signal for a current source in a given range of frequencies and amplitudes of the control signal was carried out. It has been established that the error in the amplitude of the control signal does not exceed 0.7%, and the error in the frequency of the control signal does not exceed 0.008%.

1 Introduction

To conduct research using electrical impedance tomography, there is a need for device that will allow you to control the research process, automating it as much as possible. The device must switch electrodes located on the surface of the object under study, provide the ability to measure the amplitude of electrical potentials on these electrodes, and control the amplitude, shape and frequency of the injected current source.

Thus, to implement an information-measuring system for electrical impedance tomography of biological objects, the task arises of developing a unit for collecting and transmitting measurement information, which must implement the following functions:
- provide the ability to connect one of the terminals of the current source to a common point, and the second terminal to any of the electrodes on the surface of the biological object under study (BO);
- provide the ability to measure the amplitude $\Delta\varphi_{Ai}$ of changes in potential φ_i on any of the electrodes E_i on the surface BO relative to a common point;

- control must be carried out using the control program installed on a PC, connected to a PC via a universal USB port;
- provide the ability to control the current source (amplitude, shape and frequency) through voltage.

2 Development of structural and functional electrical diagrams of a block for collecting and transmitting measurement information

The block diagram of the developed device is shown in Figure 1.

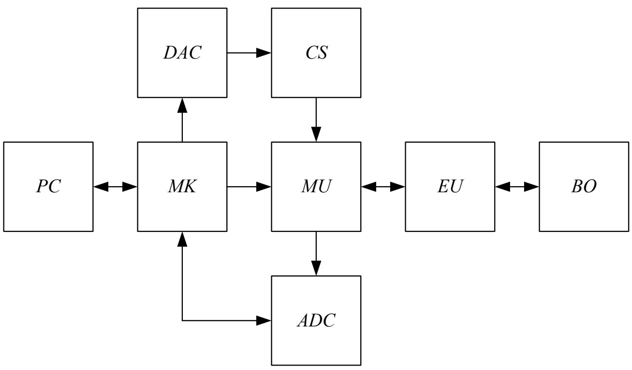

Fig.1. Block diagram of EIT device

The personal computer *PC* carries out the functions of reconstruction and visualization of the internal structure of *BO*, generates commands for the microcontroller *MK* [1], in accordance with which *MK* controls the following device blocks: digital-to-analog converter *DAC* [2], analog-to-digital converter *ADC* [2], block switching *MU*. The *DAC* converts the digital representation of the current source control signal into voltage. *ADC* converts the potential into a digital code. *MU* serves to connect *CS* [3] and *ADC* to specified electrodes. Any interaction with *BO* (injecting current *I*, measuring potential φ_i) is carried out through electrodes E_i in the electrode block.

Based on the block diagram, a functional diagram has been developed, presented in Figure 2.

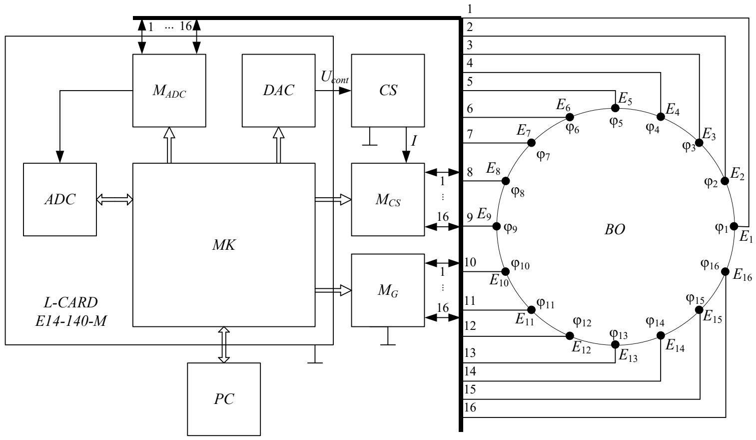

Fig.2. Functional diagram of EIT device.

The generation of control commands for *MK*, as well as the reconstruction and visualization of the internal structure *of BO* is carried out in *a PC* using the *EIT* software. Control commands are transmitted to the *MK* via a universal *USB* port. The *MK* unit controls *DAC*, *ADC* and switches using digital outputs. *The DAC* is the source of the control signal U_{cont} for the *CS* [3]. The *CS* block is connected to the specified electrodes E_i using a switch M_{CS}. The common point is connected to the given electrodes E_i using a switch M_G. Electrodes E_i are located on the surface *of BO*. Any interaction with *BO* (injection of current *I*, measurement of potential φ_i) is carried out through the electrodes E_i. The *ADC* block is connected to the specified electrodes E_i using the M_{ADC} switch. The result of measuring 5 periods [4] of the change in potential φ_i at the electrode E_i is transmitted to *MK*. The *MK* block transmits the measurement result to the *PC*. The EIT device block is implemented on the *L-CARD board E* 14-140-*MD*, which includes *MK*, *ADC* and *M*, *DAC*.

Block diagram of *EIT* device operation is presented in Figure 3.

The EIT device unit operates as follows. Experiment parameters are set in the software - frequency f_{cont}, shape and amplitude U_{Acont} control signal U_{cont} for *CS*; algorithm for obtaining data for reconstructing the internal structure of *BO*; *ADC* parameters (*ADC* conversion frequency f_{ADC}, input path gain K_{IA}, operating mode). For convenience, a comment is provided containing explanations of the experiment and a way to save the results of measuring the potential amplitude φ_{Ai} on the electrode E_i. After starting the measurement process, the software transmits the command *MK* to output code *D* to the digital outputs, controlling the switches M_{CS} and M_G [2]. After outputting code *D,* the switch M_{CS} connects the pin *CS*, and the switch M_G connects a common point to the electrodes E_i specified in the data acquisition algorithm to reconstruct the internal structure of *BO*. After this, the software transmits the initialization command to *ADC*. Initialization consists of setting the *ADC* parameters *(ADC* conversion frequency f_{ADC}, input path gain K_{IA}, operating mode). Next, using the switch M_{ADC}, the *ADC* input is connected to the electrode E_i specified in the data acquisition algorithm for reconstructing the internal structure *of BO,* and the potential φ_i is measured relative to a common point. Potential measurements φ_i are carried out on all electrodes E_i specified in the algorithm. Next, the *ADC* is turned off, the results of measuring the potential φ_i are converted from the *ADC* codes into voltage, taking into account the calibration coefficients K_{cal} and added to the array with measurement results. These actions are repeated until all measurements specified in the data acquisition algorithm for reconstructing the internal structure of *BO* have been completed. The interface for working with the EIT device is closed, the results of measuring the potential φ_i are processed in the software and saved to a text file.

 https://doi.org/10.1051/e3sconf/202346004024

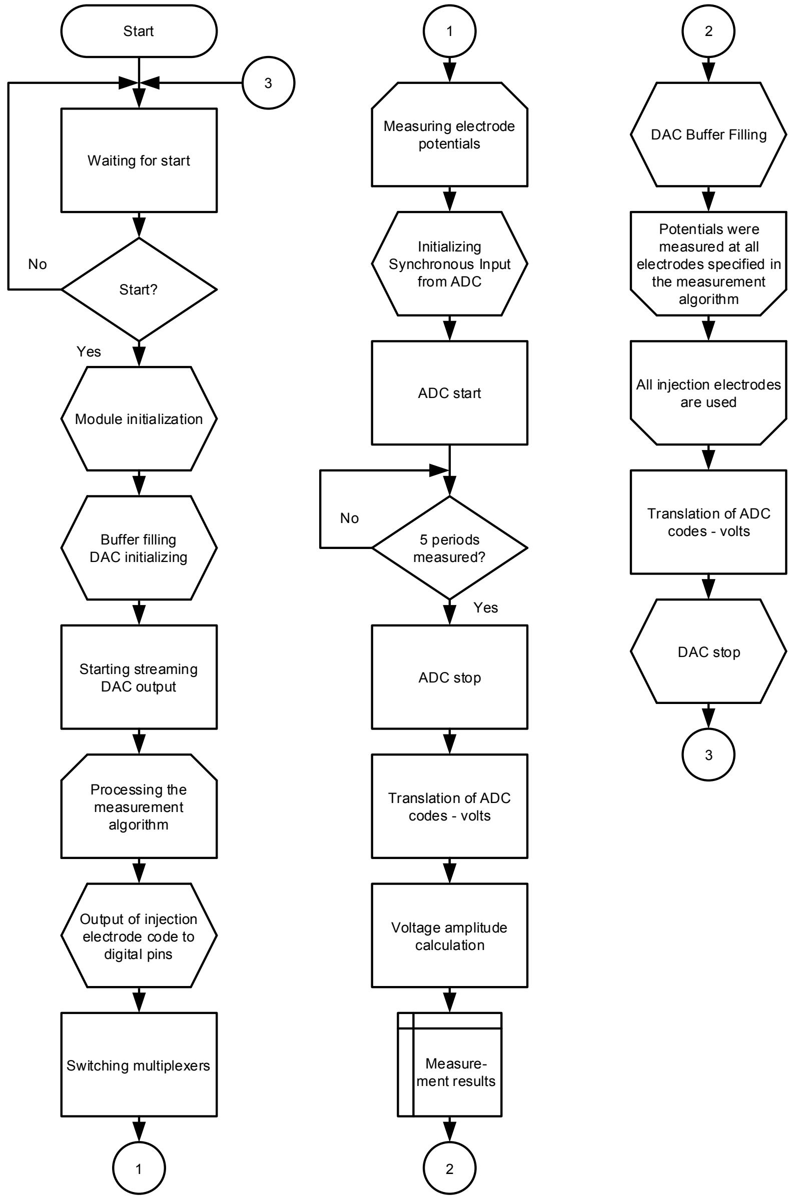

Fig.3. Block diagram of the operation algorithm of the EIT device

The following data acquisition measurement algorithm is implemented to reconstruct the internal structure of *BO*. Electrode E_1 is connected to the common point, electrode E_2 to *CS*. The potentials $\varphi_1..\varphi_{16}$ are measured on the electrodes $E_1..E_{16}$ relative to a common point. Next, electrode E_2 is connected to the common point, electrode E_3 to *CS*. The potentials $\varphi_1..\varphi_{16}$ are measured on the electrodes $E_1 .. E_{16}$ relative to a common point. And so on until electrode E_{16} is connected to the common point, and electrode E_1 to *CS*.

To build EIT device, E14-140-MD input/output board was used [5], which included *MK*, *ADC*, *DAC*, M_{ADC}. The board has the ability to be controlled from the *LabView* programming environment [6] and is low cost.

Connection diagram of EIT device blocks to *L-CARD* E14-140-MD is shown in Figure 4.

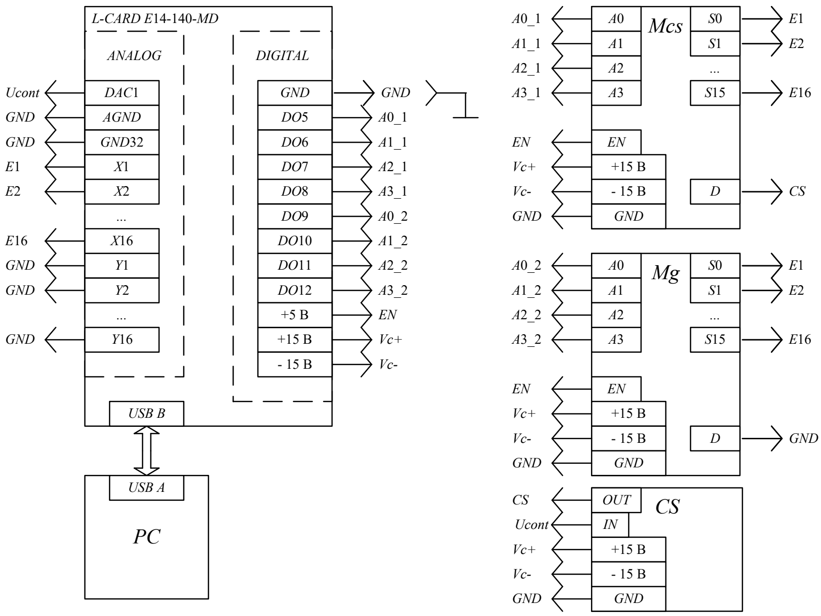

Fig.4. Connection diagram of EIT device blocks to *L-CARD E*14-140-*MD*

Based on the drawn up diagram, a switchboard was designed and created that interconnected the main blocks of the EIT device. The development was carried out in the *DipTrace* software [7]. The printed circuit board drawing is shown in Figure 5. The board assembly drawing and appearance are shown in Figure 6.

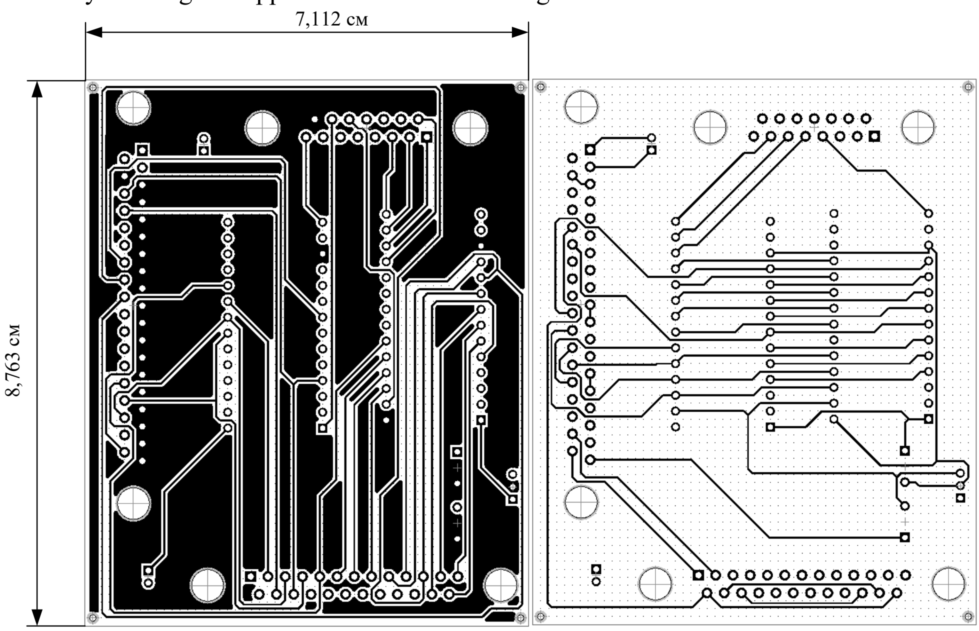

Fig.5. Printed circuit board drawing of switches

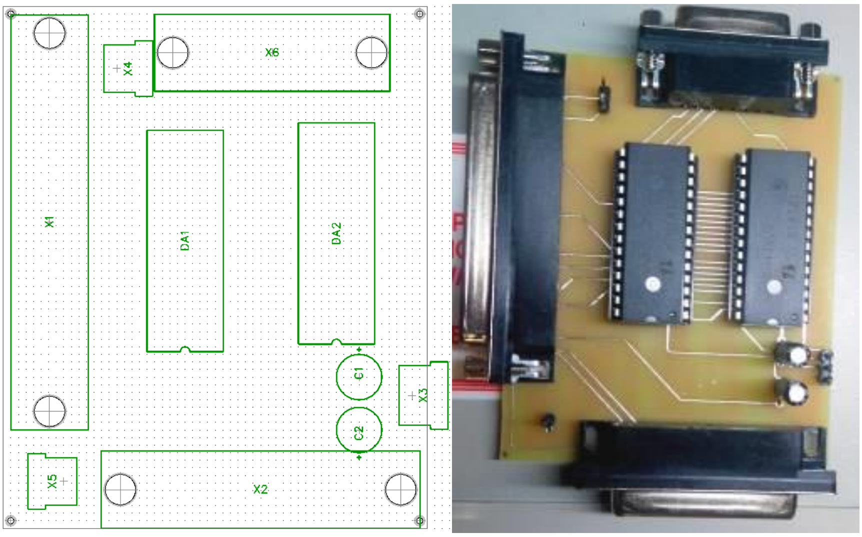

Fig.6. Assembly drawing and appearance of the switch board

The appearance of the assembled EIT device is shown in Figure 7. Thus, the main blocks of the device (current source, switch unit, and measurement data acquisition and transmission unit) are located in one case. This hardware solution connects to a PC via a USB port.

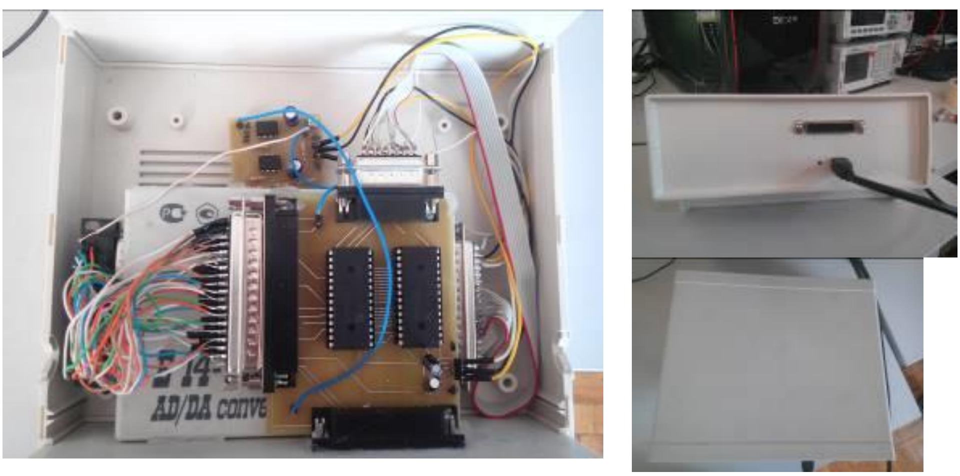

Fig.7. Appearance of the assembled EIT device

3 Experimental studies

The developed device is controlled using the *CP* control program installed on *a PC*, connected to the *PC* via a universal *USB* port. The *CP* control program was created in the *LabView* graphical programming environment from National Instruments. To test the possibility of connecting one of the terminals of the current source to a common point, and the second terminal to any of the electrodes on the surface of the biological object under study *BO* and the ability to provide measurement of the amplitude $\Delta\varphi_{Ai}$ of the change in potential φ_i on any of the electrodes E_i on the surface *BO* relative to the common point a test load was prepared, the diagram of which is presented in Figure 8. The performance of the device was also tested on a biological object.

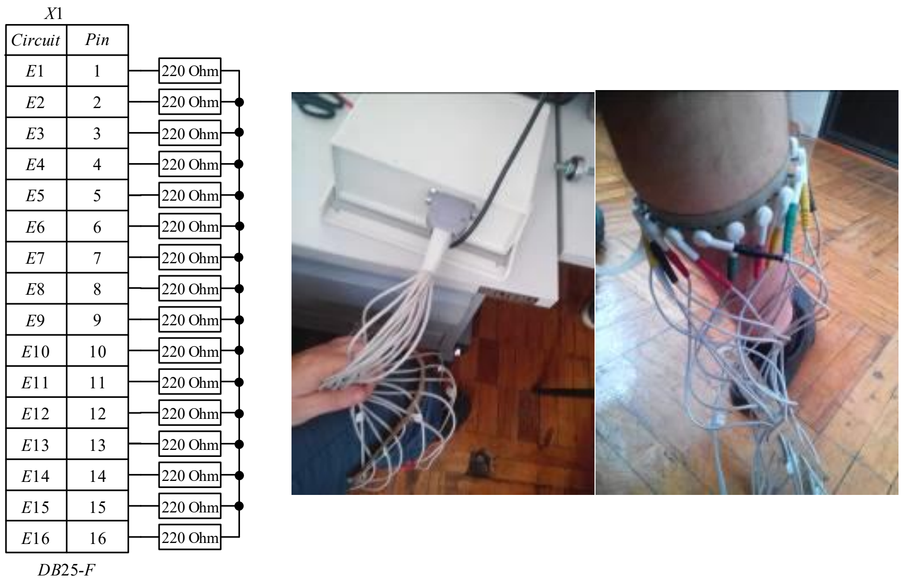

a) b)

Fig.8. Test load (a) and biological object (b)

For the specified load, with the implemented measurement circuit on the electrode E_i connected to a common point, the amplitude $\Delta\varphi_{Ai}$ of the change in potential φ_i must be equal to the voltage drop across the switch M_G. On the electrode E_i connected to the current source, the amplitude $\Delta\varphi_{Ai}$ of the change in potential φ_i should be equal to the sum of the voltage drops across the switch M_G and at the load resistance between the electrodes connected to the common point and the current source. When measuring the potential on the remaining electrodes, the amplitude $\Delta\varphi_{Ai}$ of the change in potential φ_i should be equal to the sum of the voltage drop across the switch M_G and the voltage drop across the resistance connected to the common point. With load resistor resistance R_{load} =220 Ohm and current through the load with amplitude I_m =5 mA, the amplitude of the voltage drop between the electrode connected to the common point and the electrode connected to the current source should be $\Delta\varphi_A = R_{load}$ $I_m = 2.2$ V.

Figure 9 shows a screenshot of the operation of the control program after the process of obtaining measurement data for electrical impedance tomography when connecting the test load electrode belt and the biological object to the connector.

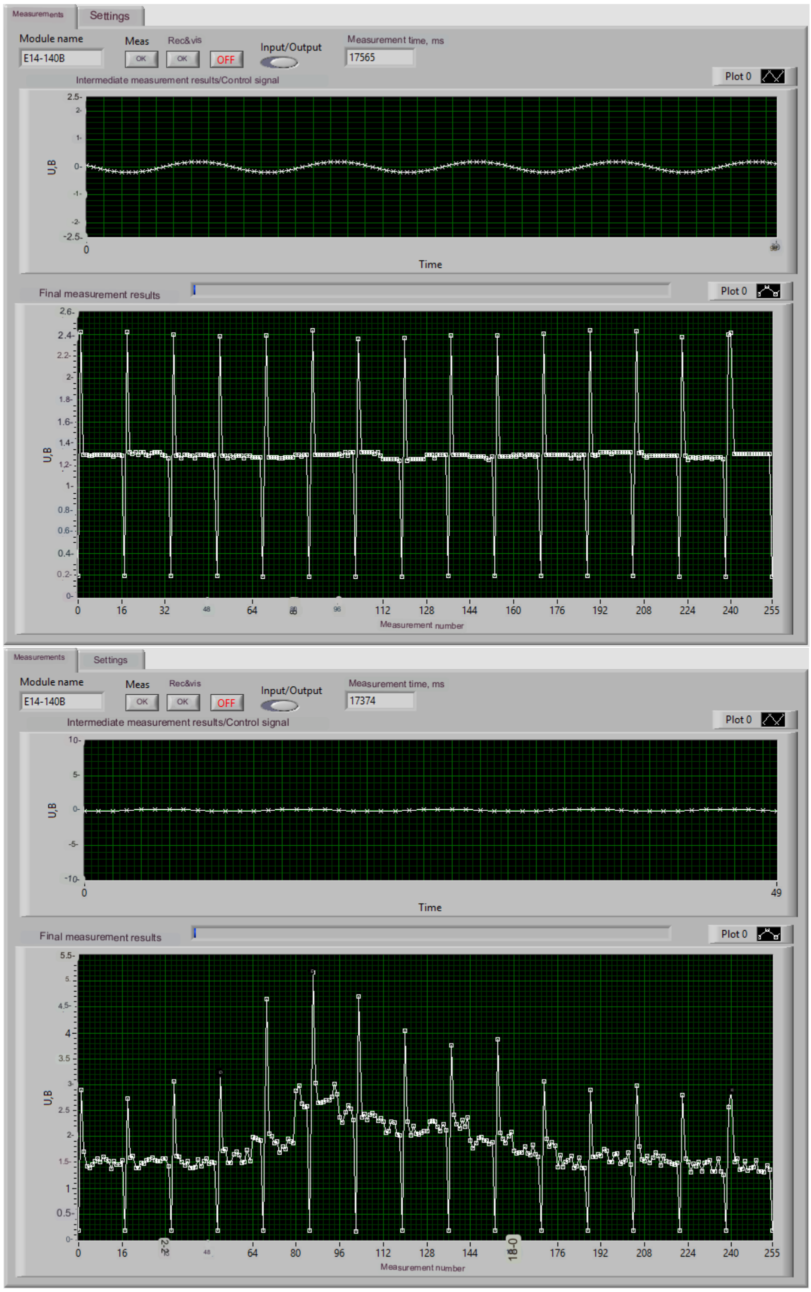

Fig.9. Screenshot of the front panel of the virtual instrument

As can be seen from Figure 9, the developed EIT device operates according to a given algorithm and allows you to connect one of the terminals of the current source to a common point, and the second terminal to any of the electrodes on the surface of the biological object under study (BO) and allows to measure the amplitude $\Delta\varphi_{Ai}$ of the change in potential φ_i at any of electrodes E_i on the *BO* surface relative to a common point.

The main parameters of current source control were also assessed:

- error δ_{cont} of the amplitude U_{Acont} of the control signal U_{cont} for *CS*;

- error δ_f frequency f_{cont} of the control signal U_{cont}.

Digital-to-analog converter *DAC* of *L-CARD E* 14-140-*MD* allows to reproduce alternating voltage in the range of ±5V with a sampling frequency f_{DAC} =200 kHz. The nonlinearity of the conversion increases at the boundaries of the range; the manufacturer's recommended output signal range is ±4.5V. According to Kotelnikov's theorem [8], it is possible to restore the original signal of frequency f with a finite spectrum by taking its discrete samples with a frequency of at least f/2. However, all real signals have an infinite spectrum. To reduce the signal spectrum, low-pass filters are used. Thus, using complex high-Q filters, it is possible to obtain a signal with a frequency f_{cont} < 100 kHz at the *DAC* output. Because there is no filter in this EIT device implementation; the signal shape at the *DAC* output was assessed. To do this, to pins *GND* 32 and *AGND* of the *L-CARD E*14-140-*MD ANALOG* connector the common point of the AKIP-4115/4A oscilloscope was connected [9], and the input of the first channel of the oscilloscope was connected to *the DAC* 1 pin of *the ANALOG connector*. Signals of various frequencies and shapes were output to the *DAC* pin. The diagram and appearance of the measuring setup are presented in Figure 10. The resulting oscillograms are presented in Figure 11.

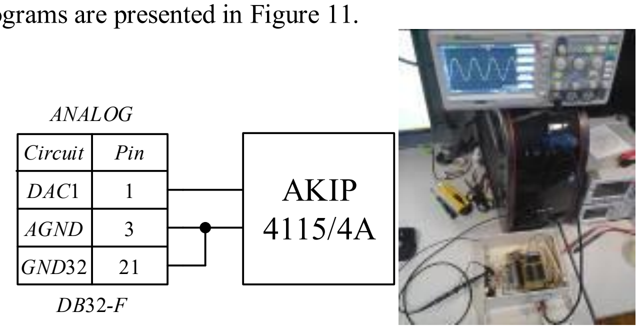

Fig.10. Connection diagram and appearance of the measuring setup

f_{cont} =1 kHz, CH1=500 mV, M=100 μs. Waveform: sine and triangle

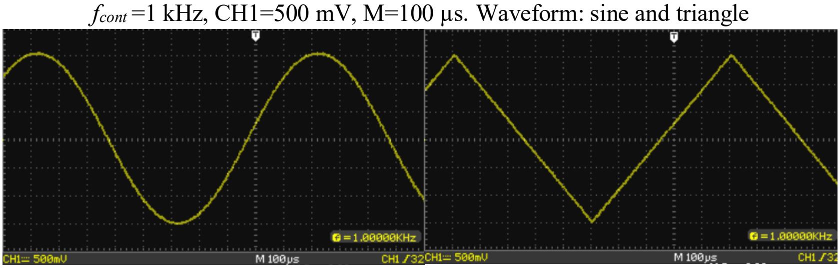

f_{cont} = 10 kHz, CH1 = 500 mV, M = 10 μs. Signal shape: sine and triangle

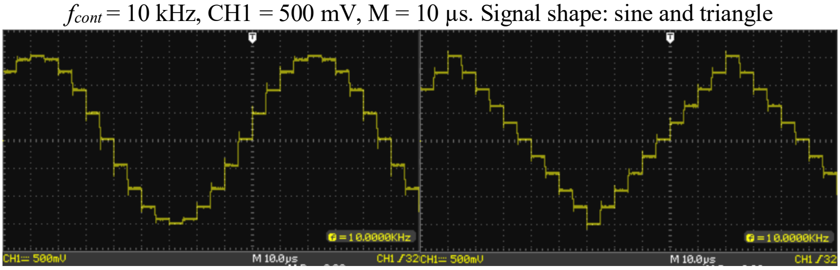

f_{cont} = 20 kHz, CH1 = 500 mV, M = 5 μs. Signal shape: sine and triangle

 https://doi.org/10.1051/e3sconf/202346004024

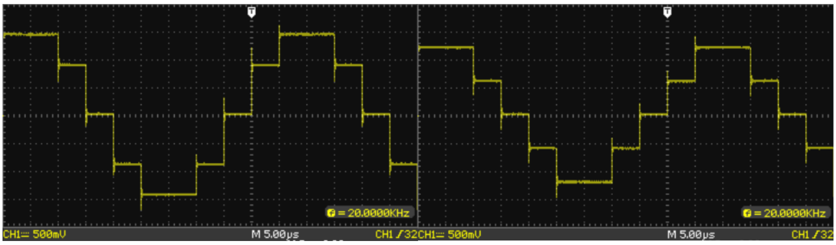

f_{cont} = 50 kHz, CH1 = 500 mV, M = 2.5 µs. Waveform: sine and square

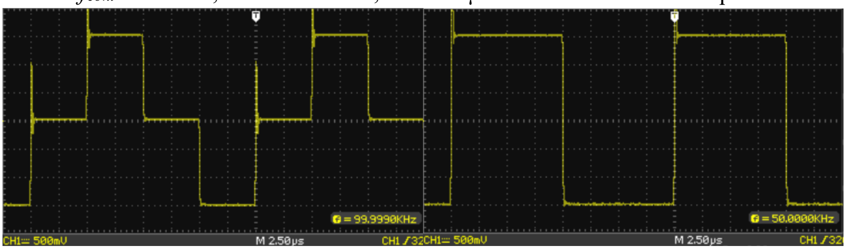

Fig.11. Oscillograms

As can be seen from Figure 11, when trying to output a signal with a frequency of f_{cont} = 20 kHz to the *DAC* output, it is impossible to distinguish between a sine wave and a triangular signal. In this case, rectangular pulses are output without distortion at a frequency f_{cont} up to 50 kHz. To solve this problem, it is possible to connect an external generator as a source of control voltage U_{cont}. In the future, it is planned to switch to the *L-card E*-503 , which includes an *ADC* with a sampling frequency f_{ADC} = 2 MHz and DAC with sampling rate f_{DAC} = 1 MHz [10]. Thus, for further research we will limit ourselves to a frequency of 15 kHz.

To estimate the error δ_{cont} of the amplitude U_{Acont} of the control signal U_{cont} for *CS*, we reproduce an alternating sinusoidal voltage with a frequency f_{cont} = 1÷15 kHz with a step of 1 kHz with an amplitude U_{Acont} = 0.22÷1.1 V with a step of 0.22 V. The selected values of the amplitude U_{Acont} of the control signal U_{cont} make it possible to obtain current *I* with amplitude I_m at the output of the current source *CS* = 1÷5 mA in 1 mA steps. To measure the amplitude U_{Acont} of the control signal $U_{cont,}$ a universal voltmeter AKIP-2101 is used [11]. The connection diagram and appearance of the measuring setup are shown in Figure 12. 11 repeated experiments were performed.

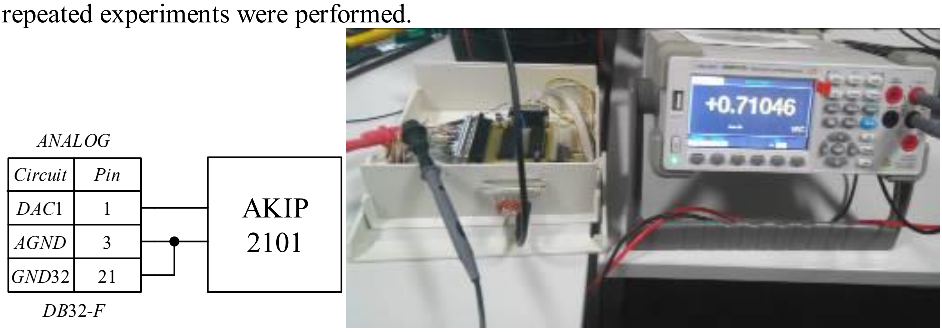

Fig.12. Connection diagram and appearance of the measuring setup

The main characteristics of voltage measurement with the AKIP-2101 voltmeter are summarized in Table 1.

Table 1. Main characteristics of voltage measurement with the AKIP-2101 voltmeter

Parameter	Value
AC voltage measurement limits	200 mV / 2 / 20 / 200 / 750 V
Permission	1 / 10 μV / 0.1 / 1 / 10 mV
frequency range	20 Hz…100 kHz
Measurement error	±0.2…3% $U_{meas.}$ +0.05…0.1% $U_{a.m.}$
Input impedance	1 MΩ / 100 pF

This voltmeter allows you to determine the effective U_{RMS} value of alternating voltage. The amplitude U_m value is calculated using the formula [4]:

$$U_m = U_{RMS} \cdot \sqrt{2},$$

where U_m is the amplitude of the alternating voltage; U_{RMS} – effective value of alternating voltage.

The reduced error is calculated using the formula [4]:

$$\delta_{cont} = \frac{U_{m\_meas} - U_m}{U_M} \cdot 100\%,$$

where U_{m_meas} is the measured value of the amplitude of the alternating voltage; U_m is the specified value of the amplitude of the alternating voltage, U_M is the maximum specified value of the amplitude of the alternating voltage.

For each series of repeated experiments, the arithmetic mean value of the error δ_{cont} of the amplitude U_{Acont} of the control signal U_{cont} was calculated. The dependence of the error on the frequency f_{cont} of the control signal U_{cont} for various values of the amplitude U_{Acont} of the control signal U_{cont} is shown in Figure 13.

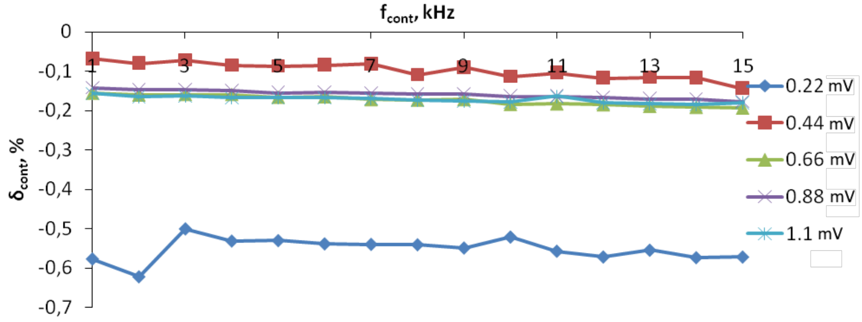

Fig.13. Result of error estimation δ_{cont}

As can be seen from Figure 13, the maximum error δ_{cont} of the amplitude U_{Acont} of the control signal U_{cont} does not exceed 0.7%.

To estimate the error δ_f of the frequency f_{cont} of the control signal U_{cont}. Let's reproduce an alternating sinusoidal voltage with a frequency f_{cont} = 1÷15 kHz with a step of 1 kHz with an amplitude U_{Acont} = 1V. To measure the frequency f_{cont} of the control signal U_{cont}, a frequency meter FM-63 is used [12]. The connection diagram and appearance of the measuring setup are shown in Figure 14. The main characteristics of the device are summarized in Table 2. 11 repeated experiments were performed.

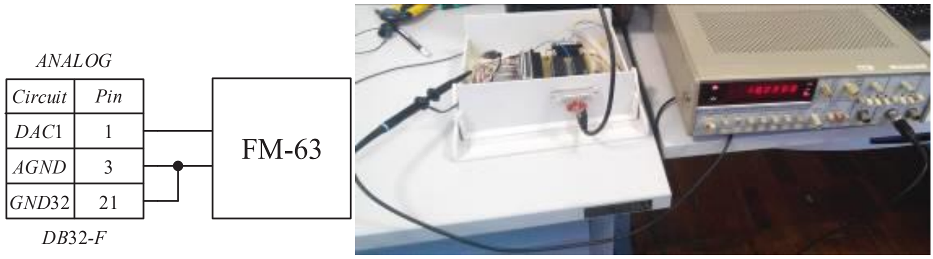

Fig.14. Diagram and appearance of the measuring setup

Table 2. Main characteristics of the frequency meter FM-63

Parameter	Meaning
Measured frequency range	0.1 Hz – 1500 MHz
Measurement error	$\pm 5\cdot10^{-7} \pm 1$ unit count.
Input impedance	1 MOhm
Input capacitance	50 pF

The error δ_f of the frequency f_{cont} of the control signal U_{cont} will be calculated according to the formula [4]:

$$\delta_f = \frac{\left| f_{meas} - f_{cont} \right|}{f_{Mcont}} \cdot 100\%,$$

where f_{meas} is the measured value of the frequency f_{cont} of the control signal U_{cont} ; f_{cont} is the specified value of the frequency f_{cont} of the control signal U_{cont}, f_{Mcon} is the maximum specified value of the frequency f_{cont} of the control signal U_{cont}.

For each series of repeated experiments, the arithmetic mean value of the error δ_f of the frequency f_{cont} of the control signal U_{cont} was calculated. Dependence of error δ_f on frequency f_{cont} of control signal U_{cont} shown in Figure 15.

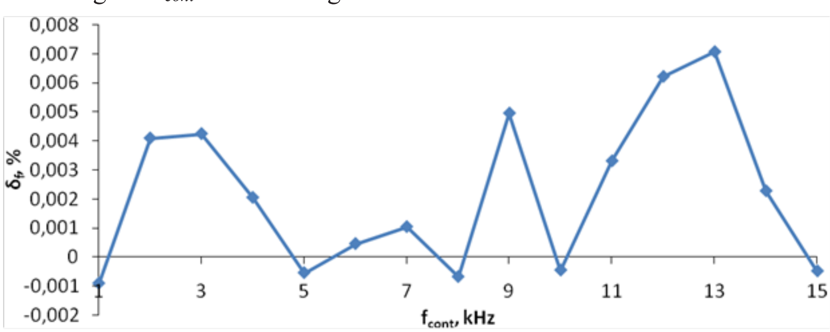

Fig.15. Result of error estimation δ_f

As can be seen from Figure 15, the maximum error δ_f of the frequency f_{cont} of the control signal U_{cont} does not exceed 0.008%.

4 Conclusion

In the course of the work, a unit for collecting and transmitting measurement information was developed for the EIT tasks. Developed device provides the ability to connect one of the terminals of the current source to a common point, and the second terminal to any of the electrodes on the surface of the biological object under study; provides the ability to measure the amplitude $\Delta\varphi_{Ai}$ of changes in potential φ_i on any of the electrodes E_i on the *BO* surface relative to a common point; control is carried out using the control program installed on the *PC*, connection to the *PC* via a universal *USB* port; it is possible to control the current source (amplitude, shape and frequency) through voltage. The accuracy of generating the control signal U_{cont} for the current source was checked at frequencies f_{cont} = 1÷15 kHz with a step of 1 kHz in the amplitude range of the control signal U_{Acont} = 0.22÷1.1 V. Error δ_{cont} of the amplitude U_{Acont} of the control signal U_{cont} does not exceed 0.7%, the frequency error f_{cont} of the control signal U_{cont} does not exceed 0.008%.

Acknowledgments

The results of the work were obtained within the framework of a grant from the President of the Russian Federation for state support of young Russian scientists MK 4856.2015.8.

References

1. Ugrjumov E.P. Digital circuitry, Saint Petersburg: BHV-Petersburg, 349-353 (2010)
2. Chizhma S.N. Electronics and microcircuitry, Moscow: FGBOU “Educational and methodical center for education in railway transport”, 111-119 (2012)
3. Titce U., Shenk K. Semiconductor circuitry, Moscow: Mir, 170-173 (1982)
4. Arhipov A.V., Zekunov A.G., Kurilov P.G., Mishin V.M., Nefedov V.A., Novikov V.A., Panov V.P. Metrology. Standardization. Certification, Moscow: JuNITI-DANA, 105-109 (2012)
5. Garmanov A.V. Devices for mobile systems E14-140 E14-140-M. User guide, Moscow: L-CARD, 2016, 34-42 (2016)
6. LabVIEW System Design Software (2015)
7. DipTrace User Guide, Novarm Ltd, 4-83 (2012)
8. Solonina A.I., Ulahovich D.A., Arbuzov S.M., Solov'eva E.B. Fundamentals of digital signal processing. Saint Petersburg: BHV-Petersburg, 225-226 (2012)
9. Arbitrary waveform generators AKIP-3409/1, AKIP-3409/2, AKIP-3409/3, AKIP-3409/4, AKIP-3409/5
10. Voltage measuring converter E-502 User's manual. Moscow: L-CARD, 4 (2016)
11. Digital universal voltmeters AKIP-2101, AKIP-2101/1
12. Electronic counting frequency meter FM-63, 4-10 (1984)